Journal of Membrane Science & Research

journal homepage: www.msrjournal.com

Research Paper

Polyurethane Mixed Matrix Membranes for Gas Separation: A Systematic Study on Effect of SiO_2/TiO_2 Nanoparticles

Manijeh Azari Monsefi [1], Morteza Sadeghi [2,*], Mohammad Ali Aroon [1,3], Takeshi Matsuura [4]

[1] *Caspian Faculty of Engineering, College of Engineering, University of Tehran, Tehran, Iran*
[2] *Department of Chemical engineering, Isfahan University of Technology, Isfahan, 84156-83111, Iran*
[3] *Membrane Research Laboratory, School of Chemical Engineering, College of Engineering, University of Tehran, Tehran, Iran*
[4] *Department of Chemical and Biological Engineering, University of Ottawa, Ottawa, Ontario, Canada K1N 6N5*

Article info

Received 2018-02-02
Revised 2018-07-14
Accepted 2018-07-24
Available online 2018-07-24

Keywords

Polyurethane
Gas separation membranes
TiO_2/SiO_2
MMMs

Highlights

- The effect of SiO_2 and TiO_2 nanoparticles on the gas separation performance of the polyurethane (PU) membranes investigated.
- The fabricated membranes characterized by FTIR, SEM and DSC analyses.
- Permeability of membranes measured using CO_2, CH_4, N_2 and O_2 gases.
- SiO_2 and TiO_2 increase permeability of all gases when used separately or in combination.

Graphical abstract

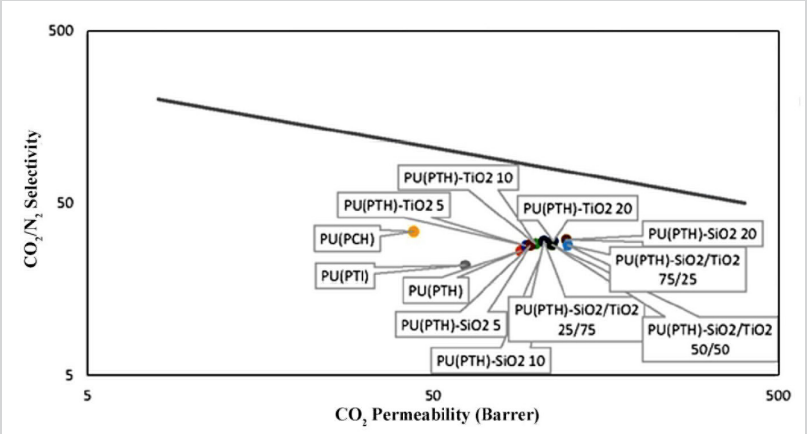

Abstract

In this study, the effect of SiO_2 and TiO_2 nanoparticles on the gas separation performance of the polyurethane (PU) membranes has investigated. Polyurethanes were synthesized by bulk two step polymerization of polytetramethyleneglycol (PTMG)/polycaprolactone (PCL): isophorone diisocyanate (IPDI)/hexamethylene diisocyanate (HMDI): 4,4'-methylenebis(2-chloroaniline) (MOCA) in mole ratios of 1:3:2. Silica nanoparticles were synthesized using the sol-gel method by hydrolysis of tetraethoxysilane (TEOS) while commercial TiO_2 nanoparticles were used. The neat PU membrane and PU-SiO_2, PU-TiO_2 and PU-SiO_2-TiO_2 flat sheet asymmetric mixed matrix membranes (MMMs) were fabricated by phase inversion and characterized by Fourier transform infrared (FTIR) spectroscopy, scanning electron microscopy (SEM) and differential scanning calorimetry (DSC) analyses. Although SEM observation showed uniform distribution of SiO_2 and TiO_2 nanoparticles inside the polymer matrix, agglomerated nanoparticles were observed at high silica contents in the MMMs of different SiO_2/TiO_2 ratios. Permeability of membrane samples were measured using pure CO_2, CH_4, N_2 and O_2 as test gases. The experimental results revealed that SiO_2 and TiO_2 could increase permeability of all gases when used separately or in combination. It was shown that when SiO_2 and TiO_2 were added in combined form, the separation performance of MMMs could be improved significantly; either permeability increased up to 120 barrer or CO_2/N_2 selectivity up to 34, although the individual effect of SiO_2 and TiO_2 on the selectivity of gas pairs was different.

1. Introduction

In order to overcome polymeric membranes permeability-selectivity trade-off [1], mixed matrix membranes (MMMs) have developed for gas separation applications [2-10]. In the MMM concept, inorganic particles (e.g. zeolites, silica, alumina, titanium dioxide, carbon molecular sieves, and carbon nanotubes) are distributed uniformly inside the polymer matrix to use their excellent separation properties along with the processability and flexibility of polymers [2, 4, 6-11]. Among the different permeable or impermeable inorganic materials used for MMMs fabrication, Silica nanoparticles have been used extensively in different polymer matrix (polyimide, polyamide, polyurethane, polysulfone, polybenzimidazole, ethyl

* Corresponding author at: Phone: +983133915645; fax: +983133912677
E-mail address: m-sadeghi@cc.iut.ac.ir (M. Sadeghi)

DOI: 10.22079/JMSR.2018.80692.1175

vinyl acetate) because of their great effect on separation properties (especially on gas selectivity), mechanical strength and thermal stability of the polymeric membranes [11-22]. For example, Pinnau et al. [22] showed that silica particles would increase the gas permeability of polysulfone membranes significantly.

In addition to silica, the researchers showed that TiO_2 impermeable nanoparticles can also affect gas separation properties of polymeric membranes drastically [23-26]. In our recent research, we prepared PU/TiO_2 MMM and evaluated its gas separation properties. Our results showed that TiO_2 nanoparticles could enhance the gas separation performance of the PU membranes [23]. Hu et al. [26] fabricated the polyimide/TiO_2 MMMs using sol-gel method and reported a significant increase in gas selectivity of test gases. Matteuci et al. [24] also studied the gas separation properties of poly(1-trimethylsilyl-1-propyne)/TiO_2 nanocomposite membranes and showed at high TiO_2 loadings the permeability of N_2, O_2 and CO_2 gases increased by nearly four times.

In MMMs fabrication, in addition to inorganic particles, which play an important role in separation and morphological properties of the resultant membranes, selection of polymer matrix, is also a key parameter. Although researchers used different kinds of glassy and rubbery polymers for MMMs preparation, rubbery polyurethanes have seldom used despite their unique properties that can be used in gas separation membranes development [27-29]. They are block copolymers consisting of urethane, or urea, hard segments and polyol soft segments. It has shown by some researchers that, gas permeability of polyurethane membranes increases as the hard segment decreases and the soft segment increase [30, 31]. Furthermore, the chemical nature of polyols and chain extenders in polyurethane polymers not only can affect crystallinity, density and the glass transition temperature of the polymer but also can change phase separation behavior, morphology and gas separation properties of the prepared membranes directly [32-38].

The effect of type and length of chain extenders, type, length and content of the soft and hard segments; the effect of the urethane and urea groups; different types of polyol, diisocyanate and chain extenders and also the effect of silica nanoparticles on morphology and separation properties of polyurethane membranes have been studied by our group earlier [14, 36, 39-40]. In the present work, the interaction effects of TiO_2 and SiO_2 on separation performance of PU (PTH) membranes (separately or in combination) has studied to find their synergic effects on each other.

2. Experimental

2.1. Materials

Polytetramethylene-glycol (PTMG, M_w=2000 g mole^{-1}) was purchased from Arak petrochemical complex (Arak, Iran). Polycaprolacton (PCL, *Mw* = 2000 g mole^{-1}) was supplied by Perstorp Co. Hexamethylene diisocyanate (HMDI), isophorone diisocyanat (IPDI), 4,4'-methylenebis(2-chloroaniline) (MOCA), Tetraethylorthosilicate (TEOS), hydrochloric acid (HCl), ethanol (EtOH), 3-glycidyloxypropyltrimethoxysilane (GOTMS) and N-dimethylformamide (DMF) were supplied by Merck. TiO_2 nano-powder with nominal size of 10-15 nm was purchased from TECNAN Co. CO_2, N_2 and O_2 gases (purity 99.99%) were purchased from Ardestan Gas Co. (Tehran, Iran) and CH_4 (purity 99.99%) was obtained from air Products Co. (Tehran, Iran).

2.2. Polyurethane synthesis

Polyurethane (PU) was synthesized by bulk two-step polymerization method as described elsewhere [33]. Briefly, PTMG or PCL has incubated with HMDI or IPDI for 2 h at 85-90ºC under nitrogen atmosphere to obtain macro-diisocyanate pre-polymer. The chain extension of pre-polymer has performed by addition of MOCA at room temperature. In order to obtain linear polymer, the molar ratio of NCO:OH was kept constant at 1:1. The molar ratios of the used components were as follows: PTMG (or PCL): IPDI (or HMDI): MOCA = 1:3:2. Table 1 shows the chemical properties and molecular structures of the materials which have been used for polyurethane synthesis. Table 2 represents the structure and thermal properties of synthesized polyurethanes.

2.3. Preparation of neat and mixed matrix membranes

Polyurethane membranes were fabricated by the solution casting solvent evaporation technique. Polyurethanes were dissolved in DMF at 70 °C to obtain a 10 wt.% homogenous solution. Then the polymer solution (dope) was poured in a petri dish and heated at 65 °C for 24 h. The obtained film was then dried in a vacuum oven at 70 °C for further 5 h to complete solvent removal.

To fabricate the TiO_2–polyurethane mixed matrix membranes, TiO_2 nano-particles were well mixed in DMF by agitation with a stirrer, and the mixture was further sonicated for 15 minutes in an ultrasonic bath to obtain a white homogenous suspension. Then a predetermined amount of polymer (PU) was dissolved in DMF and the resulting polymeric solution was added to the TiO_2/DMF suspension gradually. The polymer/nanoparticle mixture was well stirred overnight to produce a homogeneous polymeric solution containing nanoparticles. Polyurethane/TiO_2 mixed matrix membranes fabrication technique was the same as described earlier for the neat polymeric membrane fabrication. Table 3 presents dope compositions containing TiO_2 nanoparticles.

The silica (SiO_2) nanoparticles were synthesized by using sol-gel method as follows: Tetraethylorthosilicate (TEOS, 25 g) and 3-glycidyloxypropyltrimethoxysilane (GOTMS, 4g) as coupling agent was added to 30 ml ethanol (EtOH) and mixed at 70 °C for 1 hr. Then a mixture of 30 ml EtOH, 7.5 g H_2O and 0.83 g HCl was added drop wise to the TEOS/GOTMS/EtOH solution and mixed under vigorous stirring at 70 °C for 1 hr to form a clear silica sol. The silica content in the silica sol was determined by evaporating a predetermined amount of silica sol in an oven.

Silica-polyurethane suspensions were prepared by mixing different ratios of the silica sol and polyurethane-DMF solution (Table 3 for composition). It is necessary to note that during solution preparation, ethanol is evaporated and silica remains as solid inorganic dispersed phase in the polyurethane-DMF solution. Silica–polyurethane mixed matrix membranes fabrication technique was the same as described earlier for neat polymeric membrane fabrication.

Table 1
Chemicals used as the polyol, diisocyanate, and chain extenders in this study.

Unit	Chemical name	Acronym	Repetitive unit
Polyol	Polycaprolactone	PCL	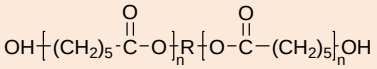
	Polytetramethylene glycol	PTMG	-(CH$_2$-CH(CH$_3$)-O)$_n$-
Diisocyanate	Isophorone diisocynate	IPDI	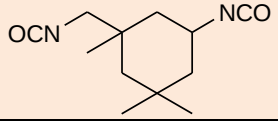
	Hexamethylene diisocyanate	HDI	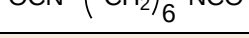
Chain extender	4,4'-methylenebis(2-chloroaniline)	MOCA	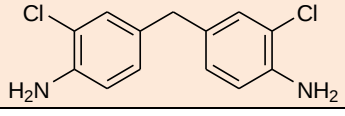

Table 2
Structure and thermal properties of the synthesized polyurethanes.

Sample Code	Components	Molar Ratio	Glass Transition Temperature (°C)
PU(PTI)	PTMG-IPDI-MOCA	1:3:2	-79
PUP(PTH)	PTMG-HMDI-MOCA	1:3:2	-79.9
PU(PCH)	PCL-HMDI-MOCA	1:3:2	-60.8

Table 3
Dope compositions of membrane samples

Sample Description		PU wt. %	TiO_2 wt. % (Solid Base)	SiO_2 wt. % (Solid Base)	TiO_2 wt. % (Total Base)	SiO_2 wt. % (Total Base)	DMF wt. %
PU(PTI), PU(PTH), PU(PCH)	Neat PU	10	0	0	0.000	0.000	90.000
PU/TiO_2	$PU/5TiO_2$	10	5	0	0.526	0.000	89.474
	$PU/10TiO_2$	10	10	0	1.111	0.000	88.889
	$PU/20TiO_2$	10	20	0	2.500	0.000	87.500
PU/SiO_2	$PU/5SiO_2$	10	0	5	0.000	0.526	89.474
	$PU/10SiO_2$	10	0	10	0.000	1.111	88.889
	$PU/20SiO_2$	10	0	20	0.000	2.500	87.500
PU/SiO_2/ TiO_2	$PU/25SiO_2/75\ TiO_2$	10	20 wt. % (TiO_2+SiO_2) (Solid Base)		1.875	0.625	87.500
	$PU/50SiO_2/50\ TiO_2$	10			1.250	1.250	87.500
	$PU/75SiO_2/25\ TiO_2$	10			0.625	1.875	87.500

SiO_2–TiO_2–PU dopes were prepared by mixing different ratios of the silica sol with TiO_2-DMF suspension and PU-DMF solution. Table 3 shows composition of polymeric solutions containing different amounts of TiO_2 nanoparticles and SiO_2 sol. It is necessary to note that the nanoparticles (SiO_2 sol+TiO_2) content was kept constant at 20 wt.% (solid base) while the weight ratios of silica sol/ TiO_2 were set at 25/75, 50/50 and 75/25 (wt./wt.). SiO_2–TiO_2 polyurethane MMM fabrication technique was as described earlier for neat and mixed matrix membranes.

2.4. Membrane characterization

2.4.1. FTIR spectroscopy

A BIO-RAD FTS-7 Fourier Transform Infrared spectroscopy was used to characterize the polyurethane (PU) and PU/SiO_2, PU/TiO_2 and PU/SiO_2/TiO_2 mixed matrix membranes at room temperature.

2.4.2. Thermal analysis

Thermal properties of the membrane samples were analyzed by differential scanning calorimeter (DSC) using Metler-Toledo DSC 822 at heating rate of 5 °C /min and the temperature range of -120 to 300 °C.

2.4.3. Scanning electron microscopy (SEM)

Morphology of the neat polymeric and mixed matrix membranes and dispersion of nanoparticles (SiO_2+TiO_2) inside the membrane were investigated using scanning electron microscopy (SEM: KYKY EM3200). All samples were cut in liquid nitrogen and coated by gold/palladium before scanning.

2.4.4. Gas permeation test

Permeabilities of the membranes were measured by using pure O_2, N_2, CH_4 and CO_2 as test gases at 10 barg of feed pressure and room temperature. A constant pressure permeation cell with effective membrane area 13.2 cm^2 was used.Eq. 1 was used to calculate the gas permeability of penetrants.

$$P = 10^{10}\frac{ql}{A(p_1 - p_2)} \quad (1)$$

where P is permeability in Barrer (1 Barrer = 10^{-10} cm^3 (STP).cm.cm^{-2}.s^{-1} $cmHg^{-1}$), q is penetrant volumetric flow rate (cm^3(STP)/s), l is the membrane thickness (cm), p_1 and p_2 are the absolute pressures of the feed side and permeate side, respectively (cmHg) and A is the effective membrane area(cm^2). The ideal selectivity, $\alpha_{A/B}$, of membranes was calculated by using Eq. 2.

$$\alpha_{A/B}=P_A/P_B \quad (2)$$

where P_A and P_B are the permeabilities of penetrants A and B respectively.

3. Results and discussion

3.1. Pure polyurethane membrane characterization

3.1.1. FTIR results

Figure 1 a shows FTIR spectra of the polyurethanes synthesized by using two different types of polyol (PTMG and PCL) and two different diisocyanates (IPDI and HMDI) and MOCA as the chain extender. As shown in Figure 1a, NCO absorption peak (at 2270 cm^{-1}) is not observable in the spectrum of all the synthesized polyurethanes; PUs (e.g. PU(PTH), PU(PTI) and PU(PCH)), which implies the completion of the polymerization reaction. The N-H stretching vibration of urethane occurs at 3313 cm^{-1} (for all PUs). The peaks at 1620-1670 cm^{-1} and 1730 cm^{-1} can be attributed to bonded and free carbonyl groups, respectively. The peak that appears at 1112-1106 $cm^{-1}$is also attributed to urethane ether linkage.

Properties of the polyurethanes (PUs) are mostly affected by the amount and micro-phase separation of the hard and soft segments [30]. On the other hand, change of the polyurethane components can affect the micro-phase separation of hard and soft segments. Therefore, the properties of the polyurethanes are directly affected by their components. Hence, in this work the effect of polyol on the structure and micro-phase separation of PUs was investigated by using two different kinds of polyols (PTMG and PCL) to find the better structure to prepare the MMM. As shown in Figure 1b, the absorption peaks of carbonyl groups in PTMG containing polyurethane (PU(PTH)) and PCL containing polyurethane (PU(PCH)) are different. It is necessarty to note that diisocyanate agent (hexamethylene diisocyanate (HMDI)) and chain extender (4,4'-methylenebis **(**2-chloroaniline**) (**MOCA**))** are the same in these two synthesized polymers.

Carbonyl group peaks in FTIR spectra can be attributed to hydrogen bonding of the urethanes hard segments, which can induce micro-phase separation of hard and soft segments. As shown in Figure 1a, the intensity of bonded carbonyl group adsorption band (1620 -1670 cm^{-1}) of PTMG

containing PU (PU (PTH)) is higher than its free form (1730 cm^{-1}). While in PCL containing PU (PU (PCH)), the free carbonyl group has an intensive peak and its bonded one is not distinctive. This effect is attributed to the formation of strong hydrogen bond between carbonyl groups and NH groups in urethane linkage of hard segments in the PTMG based polyurethane (PU (PTH)), which leads to higher phase separation in polymer. The hydrogen bonding index (HBI), the ratio of carbonyl bonds, of the studied polymers was calculated (by using Eq. 3) to examine the phase interaction.

$$HBI = \frac{A_{C=O,bonded}}{A_{C=O,free}} \quad (3)$$

where $A_{C=O,bonded}$ and $A_{C=O,free}$ are the absorbance of bonded and free carbonyl groups respectively.

The results revealed that PU (PTH) showed higher HBI value (HBI=2) than that (HBI=0.26) of PU(PCH). Existence of polar ester groups in PU (PCH) increase the capacity of hydrogen bonding between C=O groups in soft segments and NH groups in hard segments, which leads to higher phase mixing in this polymer. While PTMG containing PU, because of lack of C=O groups in its repeat unit, cannot create intersegmental hydrogen bonds as much as PU (PCH). Therefore the phase separation in PU (PTH) is more than that of PU(PCH).

To evaluate the effect of diisocyanate agent on phase behavior of PUs, two samples of PTMG based polyurethanes containing two different kinds of diisocyanates (HMDI and IPDI) were studied. As shown in Figure 1c, the absorption peak of free carbonyl group for HMDI containing polyurethane (PU(PTH)) shifted to the lower frequencies. Also, it should be noted that the bonded carbonyl's peak broadened toward lower frequencies. This phenomenon can be attributed to existence of linear aliphatic diisocyanate (HMDI) which can create more hydrogen bonds in hard segments and thus causes further micro-phase separation, whereas the IPDI containing polyurethane (PU (PTI)) has less ability to micro-phase separation because of cyclic structure of IPDI [36].

3.1.2. DSC results

Glass transition temperature (T_g) of polymeric membranes is a criterion to evaluate the chain mobility of polymers. Usually chain mobility increases as glass transition temperature decreases and vice versa. Hence, thermal properties and chain mobility of the pure polyurethane membranes synthesized in this work were analyzed by DSC results. Glass transition temperature of PU (PTH), PU (PCH) and PU(PTI) is reported in Table 2.

As shown in Table 2, glass transition temperatures (T_g) of PTMG containing PUs(PU(PTI) and PU(PTH)) are nearly the same (-79 and -79.9 ºC) while glass transition temperature of the PCL containing PU (PU(PCH)); -60.8 °C; is higher than that of PTMG containing PUs. This confirms that the chain mobility of the PCL containing PU is less than that of PTMG containing PUs. As discussed earlier in FTIR results, PTMG containing PUs undergo more phase separation in their hard and soft segments, which leads to a higher chain mobility of PTMG soft segments in polymer. Therefore, the DSC results are in accordance with the FTIR results. Considering above discussions, one can conclude that in contrast to diisocyanate agents (e.g. IPDI and HMDI), polyols (here PTMG and PCL) can affect thermal properties of polyurethane drastically.

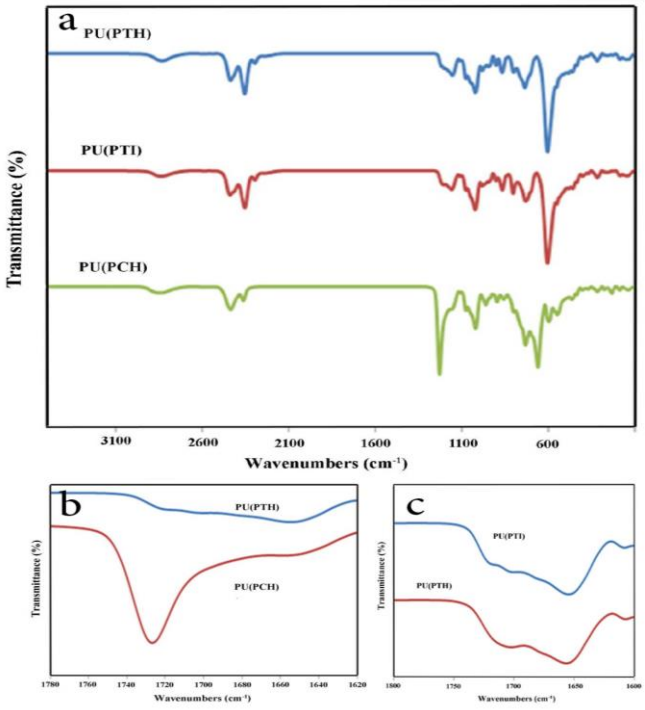

Fig. 1. (a) FTIR spectra of pure polyurethanes, (b) FTIR spectra of PU(PTH) and PU(PCH) in the carbonyl stretching range, (c) FTIR spectra of PU(PTH) and PU(PTI) in the carbonyl stretching range.

Table 4
Gas separation properties of PUs.

Pressure (barg)	Permeability (Barrer)				Ideal selectivity		
	CO_2	CH_4	O_2	N_2	$\alpha_{CO2/N2}$	$\alpha_{CO2/CH4}$	$\alpha_{O2/N2}$
PU(PTH)							
4	85.76	10	9.96	3.72	23.05	8.57	2.67
6	88.7	10.41	9.17	3.51	25.27	8.52	2.61
8	83.4	10.63	8.92	3.17	26.31	7.84	2.81
10	89.79	11.79	9.43	3.23	27.80	7.61	2.92
PU(PTI)							
4	59.56	6.8	7	2.2	27.07	8.75	3.18
6	60.53	7.36	6.9	2.3	26.32	8.22	3
8	61.5	7.5	7.1	2.88	21.35	8.2	2.46
10	62.07	7.63	7.15	2.86	21.70	8.13	2.5
PU(PCH)							
4	40.57	2.67	3.81	1.16	34.97	15.19	3.28
6	43.17	2.81	3.60	1.06	40.73	15.36	3.39
8	43.59	3.4	3.93	1.1	39.63	12.82	3.57
10	44.03	3.41	3.28	1.29	34.13	12.91	2.54

3.1.3. Gas permeation test results

Separation properties of neat polyurethane membranes (PU(PTH), PU(PTI) and PU(PCH)) were investigated at 30 °C and 4-10 barg using pure O_2, N_2, CO_2 and CH_4 as test gases. As shown in Table 4, the gas permeability of the PU(PTH) membrane is higher than that of the PU(PCH) membrane.

This can be due to the polyol and the diisocyanate used to synthesize this polymer. As discussed earlier and confirmed by FTIR and DSC results, in comparison to PCL, using PTMG as polyol can increase the phase separation between soft and hard segments, which implies higher chain mobility and greater penetrant diffusivity and permeability. Also gas permeability of HMDI containing polyurethane (PU(PTH)) is more than IPDI containing one (PU(PTI)). This effect is in accordance with FTIR and DSC results and can be explained by comparing diisocyanate structure of the PU(PTH) and PU(PTI). As discussed earlier in FTIR results, changing diisocyanate structure from aromatic (IPDI) to aliphatic (HMDI), increases the hydrogen bonds in hard segments and thus causes further micro-phase separation, which leads to an increase in chain mobility, a decrease in glass transition and an increase in gas penetrants permeability. Table 4 shows the PCL containing polyurethane membrane has the highest selectivity for all gas pairs under consideration (CO_2/N_2, CO_2/CH_4 and O_2/N_2). It can be interpreted by the least phase separation behavior and the least chain mobility of the PU(PCH) membranes. Although the decrease in chain mobility will decrease the permeabilities of both small and large penetrants, the latter permeability is affected more strongly (see Table 4, columns 2-5), yielding higher selectivities for the gas pairs (small/big). In other words, since the chain mobility of soft segments of the PCL containing PU is lower than the other ones, PU(PCH) membrane acts as the membrane of the highest selectivity and is expected to separate gas pairs most effectively (Table 4, columns 6-8). In order to select the best polyurethane for further investigation of mixed matrix membrane, CO_2/N_2 selectivity and CO_2 permeability of the synthesized polyurethanes were depicted on Robeson's upper bound plot (revisited 2008) [1]. As shown in Figure 2, among different polyurethanes synthesized in this work, PU (PCH) and PU (PTH) are located closest to Robeson's upper bound. Between these two polyurethanes, PU (PTH) was selected for MMMs fabrication due to its higher permeability.

3.2. Mixed matrix membranes characterization

3.2.1. PU (PTH)-TiO_2MMMs characterization

Chemical properties of the pure titanium dioxide (TiO_2), PU(PTH) membrane and TiO_2 containing MMMs were characterized by FTIR analysis. The results are shown in Figure 3a.

As could be observed in Figure 3a, an intensive peak is observable at 600 cm^{-1} which can be interpreted by Ti-O-Ti asymmetric stretching in pure titanium dioxide. This peak is also distinguishable in MMMs spectra (except pure PU(PTH)). Figure 3a shows that the band at 600 cm^{-1} increases as TiO_2 content in MMMs increases and it can be attributed to the presence of a broad band associated with the vibration of the Ti-O-Ti bond.

Further investigation on the effect of TiO_2 nanoparticles on PU(PTH) polyurethane chemical structure was done by FTIR analysis of the N-H stretching region of the PU(PTH) and PU(PTH)-TiO_2 membranes.

As could be observed in Figure 3b, the urethane N-H groups of the MMMs shifted to the lower frequencies in the presence of TiO_2. This is probably due to the formation of hydrogen bonding between hydrogen donner NH groups and hydrogen acceptor (e.g. Ti-O-Ti and Ti-O-H) in TiO_2 nanoparticles. The hydrogen bonding enhances the adhesion between the nanoparticles (TiO_2) and polymer matrix [18].

Morphology and distribution of nanoparticles (TiO_2) inside the polymer matrix of a mixed matrix membrane (PU(PTH)-TiO_2 20wt.%)) was investigated by scanning electron microscopy (SEM). Figure 4(a,aa) shows the cross sectional SEM micrographs of the PU(PTH)-TiO_2 20 wt.% mixed matrix membrane.

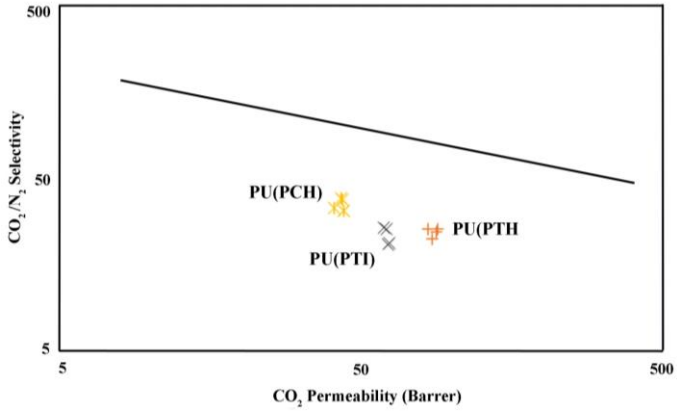

Fig. 2. CO_2/N_2 separation property of different synthesized polyurethanes in comparison to Robeson's upper bound.

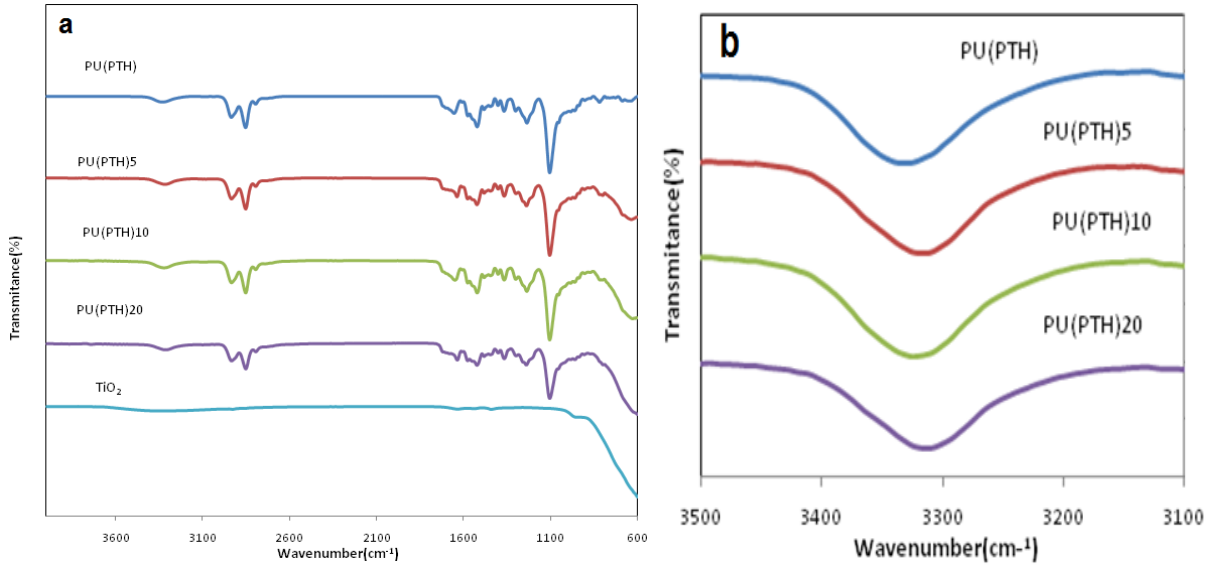

Fig. 3. (a) FTIR spectra of PU(PTH),TiO_2 and PU(PTH)-TiO_2 membranes (5, 10 and 20 numbers represent TiO_2 wt. % (solid base) in the MMMs), (b) FTIR spectra of PU(PTH) and PU(PTH)-TiO2 MMMs in the N-H stretching region (5, 10 and 20 numbers represent TiO_2 wt. % (solid base) in the MMMs).

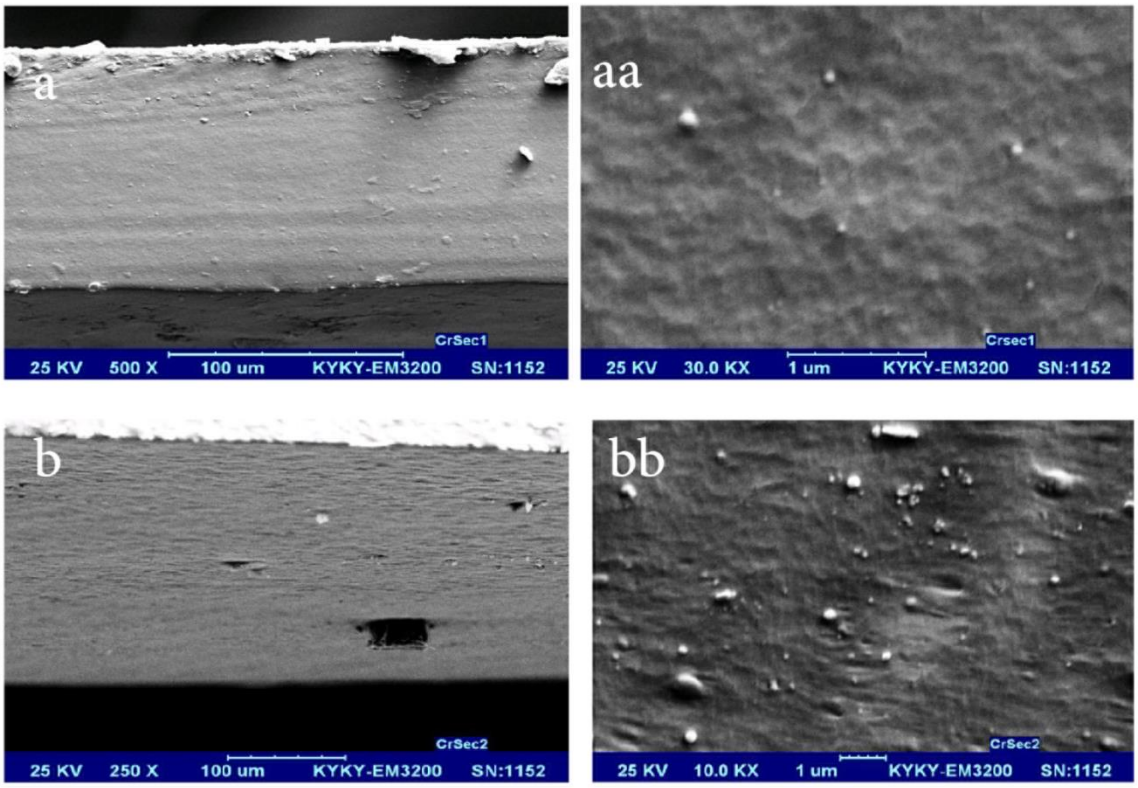

Fig. 4. (a,aa) SEM cross-sectional microphotographs (different magnifications) of the PU(PTH)- TiO_2 20 wt.% MMM, (b,bb) Cross sectional SEM micrographs of the PU(PTH)-SiO2 20 wt. % MMMs.

As shown in Figure 4a, the fabricated mixed matrix membrane is dense and completely symmetric, and no voids or defects are distinguishable between polymer matrix and nanoparticles. High magnification cross-sectional SEM (see Figure 4aa) shows good distribution of TiO_2 nanoparticles. It is necessary to note that the agglomerates of TiO_2 nanoparticles are hardly observable inside the polymer matrix (see Figure 4aa). This is due to the enhanced adhesion between the polymer chains and TiO_2 nanoparticles as proved earlier by FTIR analysis.

Figure 4(b, bb) shows the SEM micrographs of PU(PTH)-SiO_2 MMM containing 20 wt.% SiO_2.

As shown in Figure 4b, fabricated membrane is totally dense and symmetric. Good distribution of SiO_2 nanoparticles in the polymer matrix is distinguishable at high magnification images (see Figure 4bb). 10000 times magnification (see Figure 4bb) obviously demonstrates the presence of nano-sized SiO2 particles in the polymer matrix. In contrast to MMM containing TiO_2 nanoparticles, agglomerated silica particles in polymer are also observable at high magnification micrographs. This phenomenon can be due to the lower interaction between SiO_2 and polymer chains, in comparison to TiO_2 distribution in polymer.

DSC analysis was carried out to investigate the thermal properties of the PU(PTH) and PU(PTH)-TiO_2 and PU(PTH)-SiO_2 and PU(PTH)-SiO_2(50)-TiO_2(50) membranes. Table 5 presents the glass transition temperature of the PU(PTH) and PU(PTH)-TiO_2 and PU(PTH)-SiO_2 and PU(PTH)-SiO_2(50)-TiO_2(50) membrane samples.

As shown in Table 5, glass transition temperatures of the mixed matrix membranes are nearly equal to or lower than that of the neat polyurethane membrane. This indicates that the mobility of chains in soft domains increased by TiO_2 loading in polymer matrix, which can be caused by either the increase of phase separation and lower soft-hard chain interactions [22, 42]. As it already discussed, in SEM and FTIR results, because of the hydrogen bonds between NH groups of urethane and TiO_2 nanoparticles, a strong interaction between nanoparticles and polymer chains is formed in hard domains. This interaction and proper distribution of nanoparticles inside the polymer increase the phase separation of hard and soft domains, which can lead to increase the free volume in polymer. The increase of free volume provides more space for chain motion and ultimately results in the decrease of glass transition temperature [16, 22]. The interaction between NH groups of urethane and TiO_2 nanoparticles decreases the available NH groups required for formation of hydrogen bonding with ethereal groups of soft segments, hence the soft segments mobility increases due to the decrease of hydrogen bonds with hard segments and subsequently leads to the decrease of the glass transition temperature of polymer. The DSC results and decrease in the glass transition temperature of the MMMs containing nanoparticles are consistent with FTIR analysis, which showed the interactions between TiO_2 and NH groups of urethane and enhanced phase separation of hard and soft segments.

Permeabilities of the PU(PTH) and PU(PTH)-TiO_2 membrane samples were measured at 10 barg and 30 °C using pure nitrogen, methane, oxygen and carbon dioxide as test gases. Figure 5 shows gas permeability of the neat PU(PTH) and TiO_2 containing PU(PTH) membranes as a function of TiO_2 content.

As could be observed in Figure 5, permeability of CO_2 is considerably higher than that of the other gases in all membrane samples. It can be due to the high condensability, the small kinetic diameter, and more interaction of this polar gas with polar groups in the polymer [15, 17].

Table 5
Glass transition temperature of the PU (PTH) and PU (PTH)-TiO_2 and PU(PTH)-SiO_2 and PU(PTH)-SiO_2(50)-TiO_2(50) membrane samples.

Sample description	Glass transition temperature (°C)
PU(PTH)	-79.1ºC
PU (PTH)- TiO_2(5wt.%)	-83.3ºC
PU (PTH)-TiO_2 (20wt. %)	-80ºC
PU (PTH)-SiO_2 (5 wt. %)	-81.1
PU (PTH)-SiO_2 (20 wt. %)	-79.9
PU(PTH)-SiO_2(50)-TiO_2(50)	-80.5

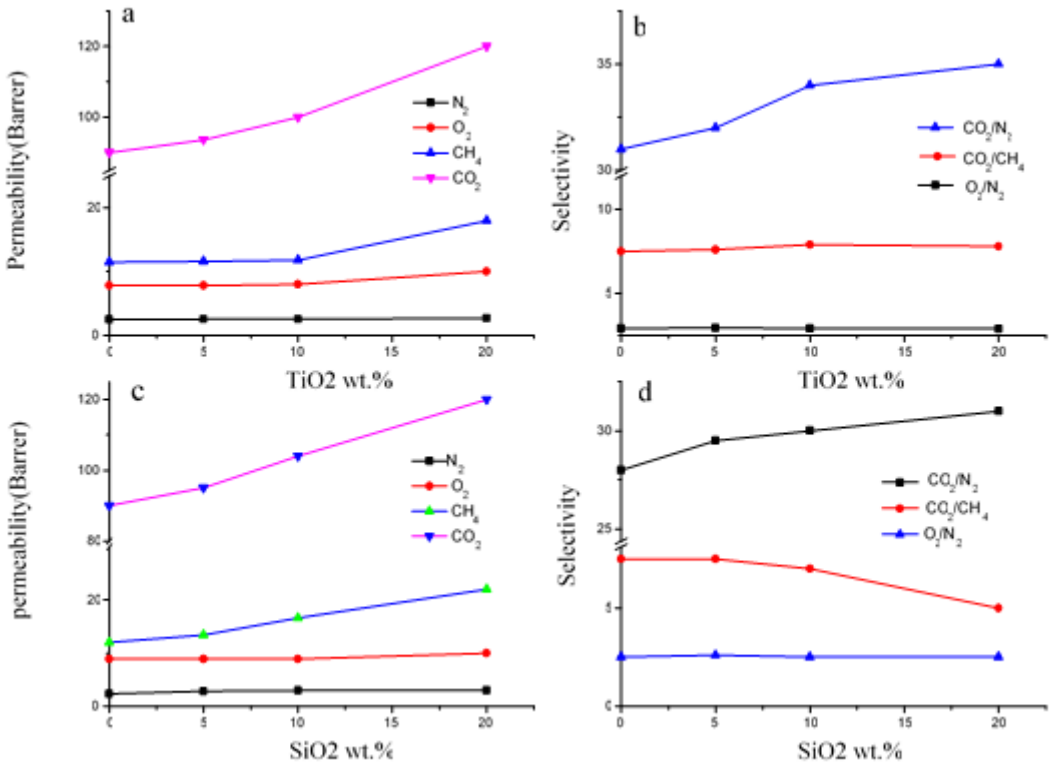

Fig. 5. (a) Gas permeability of the neat PU(PTH) and PU(PTH)-TiO_2 membranes,(b) Ideal selectivity of the neat PU(PTH) and PU(PTH)-TiO_2 membranes, (c) Gas permeability of the PU (PTH) and PU (PTH)-SiO_2 membranes, (d) Ideal selectivity of PU(PTH) and PU(PTH)-SiO_2 membranes.

Moreover, methane permeability is higher than that of oxygen and nitrogen despite of its bigger kinetic diameter. This phenomenon is due to the higher condensability of methane in comparison with nitrogen and oxygen gases. Therefore, one can confirm that the dominant mechanism for gas permeation through rubbery polymers (PU(PTH)) is solution mechanism as discussed elsewhere [28].

Figure 5a shows that permeability of the penetrants increases as TiO_2 content increases in MMMs. For example permeabilities of the N_2, O_2, CH_4 and CO_2 increase by 14 %, 11 %, 17 % and 24 % respectively as TiO_2 content increases from zero to 20 wt. %. This can interpret as follows. As it already discussedin FTIR analysis, more soft and hard segment phase separation is expected due to polar interactions between TiO_2 nanoparticles and -NH groups in hard segments, weakening the intermolecular hydrogen bonds. Phase separation makes the polymer chain segment more mobile, which results in a decrease in glass transition temperature and an increase in gas permeabilities.

Among different gases, permeability of CO_2 increases more than the other gases most likely because:

1. The interaction between residual OH groups on the surface of TiO_2 nanoparticles and CO_2 increases its solubility in mixed matrix membrane.
2. TiO_2 nanoparticles in the polymer matrix increase free volume in the region surrounding the nanoparticles, which allows CO_2 of the smallest molecular size to diffuse readily through the membrane matrix.

Figure 5b shows ideal selectivity of the PU(PTH) polymeric membranes containing different amounts of TiO_2 nanoparticles.

As shown in Figure 5b, CO_2/N_2 selectivity increases as TiO_2 content increases while the selectivities of CO_2/CH_4 and O_2/N_2 are nearly constant. The increase in CO_2/N_2 selectivity can be due to the small molecular size of CO_2 and its high solubility in membranes, caused by its interactions with polar OH groups on TiO_2 surface. On the other hand, CO_2/CH_4 and O_2/N_2 selectivity remains nearly constant most likely due to the similar thermodynamic behaviour of the gaseous components involved in each gas pair [41]. That is, both CO_2 and CH_4 are condensable while O_2 and N_2 are non-condensable. Moreover, the effects of TiO_2 nanoparticles on their permeabilities are nearly the same.

3.2.2. PU(PTH)-SiO_2 MMMs characterization

FTIR spectra of the PU(PTH) and the PU(PTH)-SiO_2 membranes are presented in Figure 6a. The most intensive peak at 1107 cm^{-1} in Figure 6a represents the Si-O-Si asymmetric stretching in the PU(PTH)-SiO_2 mixed matrix membranes. Also symmetrical vibrations peak of Si-O-Si at 820 cm^{-1} is observable in all MMMs.

To investigate the interaction between silica nanoparticles and PU(PTH) polymer, N-H stretching regions were studied more in detail. As shown in Figure 6b the most intensive peak at 3342 cm^{-1} for PU(PTH), which represents N-H stretching, shifts gradually as the SiO_2 content increases and reaches finally 3325 cm^{-1}. This phenomenon can be attributed to the formation of hydrogen bonding between N-H groups in PU(PTH) hard segment and OH groups on silica nanoparticle surfaces. Therefore, one can expect a good distribution and dispersion of silica nanoparticles in polymer matrix [18].

As shown in Table 5, glass transition temperature (T_g) of MMMs containing 5 and 20 wt. % SiO_2 nanoparticles are slightly lower than that of neat PU(PTH) membrane. The decreases in T_g of the MMMs can be attributed to the increase in polymer chains mobility. As was discussed earlier, SiO_2 nanoparticles can form hydrogen bonds with NH groups of PU(PTH) and it causes a suitable distribution of SiO_2 nanoparticles inside the polymer matrix. The good distribution of SiO_2 nanoparticles inside the polymer and their interactions with polymer chains cause them to stay between polymer chains and consequently an increase in the free volume (appropriate space for polymer chains to move freely) is expected. As a result, chain mobility increases and glass transition temperature decreases. Moreover, the interactions between NH groups of PU(PTH) polyurethane and OH groups on silica surfaces can decrease the NH groups needed for hydrogen bonds formation with ethereal groups in soft segment and, as a result, the soft segments mobility increases [21]. With increasing phase separation in polymer and decreasing physical bonds between soft and hard segments, the chain mobility in soft segments of polyurethane is enhanced, which leads to an increase of amorphous region in MMMs [16, 42, 43], resulting in decrease in the glass transition temperature.

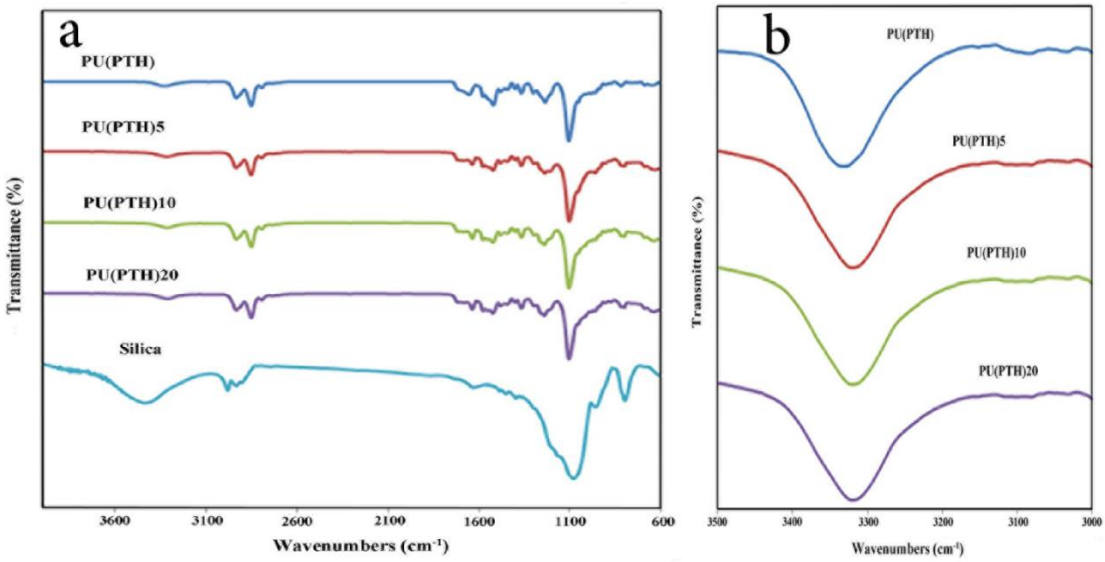

Fig.6: (a) FTIR spectra of PU(PTH) and PU(PTH)-SiO_2 membranes (5, 10 and 20 numbers represent SiO_2 wt. % (solid base) in the MMMs), (b) The FTIR spectra at N-H stretching region for PU(PTH)-SiO_2 MMMs (5, 10 and 20 numbers represent SiO_2 wt. % (solid base) in the MMMs).

Permeabilities of N_2, O_2, CH_4 and CO_2 gases through PU(PTH) and PU(PTH)-SiO_2 membranes were measured at 30 °C and 10 barg. The permeability results are shown in Figure 5c.

As shown in Figure 5c, permeability of CO_2 is higher than that of the other gases. As mentioned earlier the high permeability of CO_2 is due to its small kinetic diameter and its high condensability. In addition, interaction between this polar gas (CO_2) and polymer polar groups and OH groups on silica nanoparticle surfaces makes CO_2 more permeable.

As could be observed in Figure 5c, permeabilities of all test gases increase as silica content increases in MMMs. For example, permeabilities of N_2, O_2, CH_4 and CO_2 gases in the PU (PTH) membrane containing 20 wt.% SiO_2 are, respectively, 22 %, 15%, 112% and 36% more than those in neat PU(PTH) membrane. Gas permeability increased by incorporation of SiO_2 nanoparticles for the same reason as incorporation of TiO_2 nanoparticles.

The greater permeability increase of condensable gases (CO_2 and CH_4) than non-condensable ones (N_2 and O_2) by the addition of SiO_2 nanoparticles is also for the same reason as the addition of TiO_2 nanoparticles.

Ideal selectivity of PU(PTH) and PU(PTH)-SiO_2 membrane samples is presented in Figure 5d. As could be observed in the Figure 5d, in comparison to the neat PU(PTH) membrane, selectivities of CO_2/N_2 in MMMs containing silica nanoparticles increase as silica contents increase. O_2/N_2 selectivity of the MMMs is also higher than that of the neat PU (PTH). In contrast to PU(PTH)-TiO_2 MMMs, PU(PTH) containing SiO_2 nanoparticles have CO_2/CH_4 selectivities less than that of neat PU(PTH) membrane. The increase in CO_2/N_2 selectivity can be due to the smallest molecular size of CO_2, its high solubility and its interaction with the functional groups of polymer and SiO_2 nanoparticles as discussed earlier. As shown in Figure 5d, the CO_2/CH_4 selectivity increases slightly as SiO_2 increases by 5 wt.% and then it decreases as the nanoparticle content increases from 5 to 20 wt.%. The increase in permeability of CH_4 and the decrease in CO_2/CH_4 selectivity in MMMs containing a large amount of SiO_2 nanoparticles are attributed to the agglomeration of SiO_2 nanoparticles (as discussed earlier in SEM results) and the formation of Knudsen size interfacial voids around them. The slight increase in O_2/N_2 selectivities of the MMMs from silica content of 0 to 5 wt.% is most likely because of the non-condensability behavior of O_2 and N_2 gases, which makes their separation to be controlled by their molecular size. On the other hand, the diffusion pathways in the polymer matrix, which increases as silica content increase, control the diffusivity of penetrants in the MMMs. Therefore the smaller molecule (O_2) diffuses more rapidly than the larger one (N_2) and O_2/N_2 selectivity of PU(PTH) membrane increases by addition of SiO_2 nanoparticles to the polymer matrix. As well, The O_2/N_2 and CO_2/CH_4 selectivities decrease when the silica loading becomes as high as 20 wt. %. This can be attributed to SiO_2/PU(PTH) interface defects which likely create small voids at the polymer-nanoparticle interface.

3.2.3. PU(PTH)-TiO_2-SiO_2 MMMs characterization

As shown in Figure 7, both TiO_2 and SiO_2 nanoparticles can improve gas separation properties of PU(PTH) membranes. Therefore one can expect that combination of TiO_2 and SiO_2 nanoparticles also improve performance of PU(PTH) membranes.

Figure 7 shows that PU(PTH) MMMs containing 20 wt. % TiO_2 and SiO_2 nanoparticles have the best performance (e.g. the highest permeability and selectivity) for CO_2/N_2 separation. Hence 20 wt. % (solid base) nanoparticles (TiO_2 +SiO_2) loading is chosen for further discussion to investigate the interaction effects of TiO_2 and SiO_2 on separation properties of PU(PTH) membranes. It is necessary to note that although the total nanoparticles (TiO_2 +SiO_2) content was kept constant at 20 wt. % various SiO_2/TiO_2 ratios (25/75, 50/50 and 75/25 wt. %/wt. %) were used.

FTIR spectra of PU(PTH) and PU(PTH)-TiO_2-SiO_2 membrane samples are shown in Figure 8a. As could be observed (see Figure 8a), the most intensive peak at the frequency of 1109 cm^{-1} represents the asymmetric Si-O-Si bonds in the MMMs. In addition, the peak at 600 cm^{-1} is attributed to TiO_2 nanoparticles in the PU(PTH)-TiO_2-SiO_2 MMMs. It is obvious that this peak is intensified as the TiO_2 content increases in the membranes.

As shown in Figure 8b, there is no notable change between the NH spectrums of the three prepared membranes.

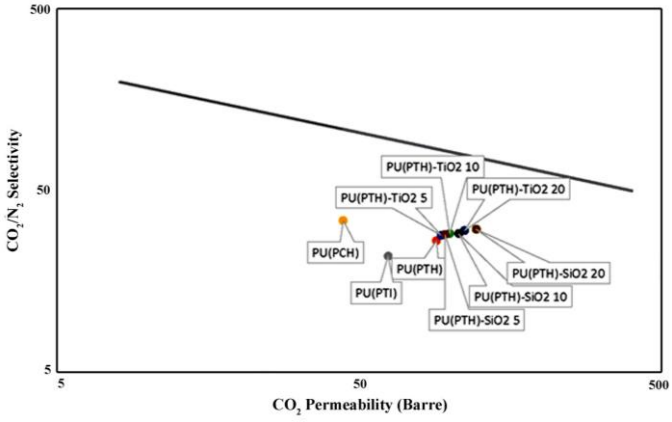

Fig. 7. CO_2/N_2 separation properties of PU(PTH) MMMs containing SiO_2 and TiO_2 nanoparticles on Robeson's upper bound plot.

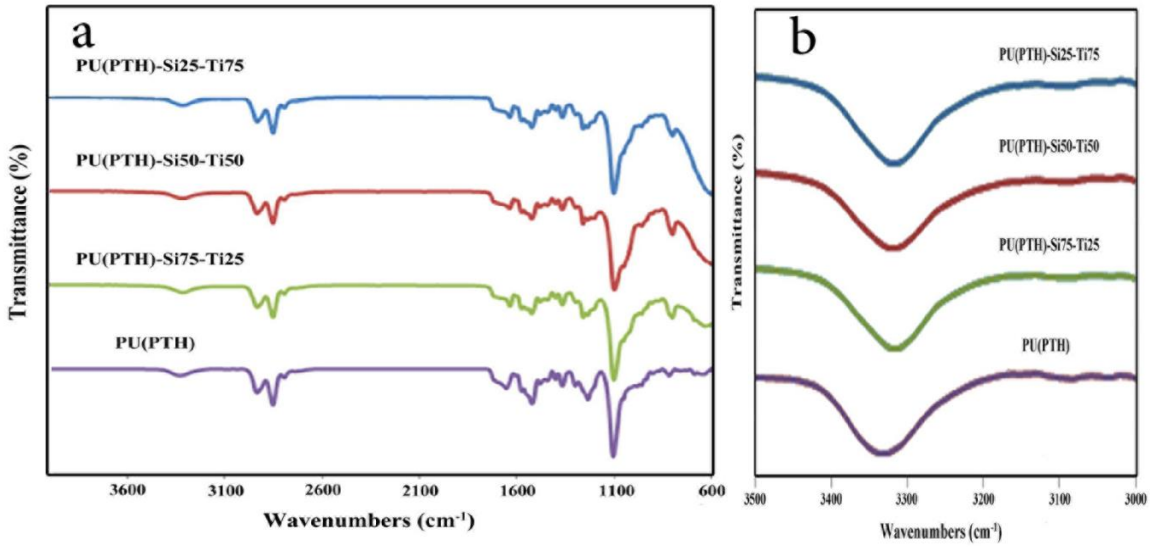

Fig. 8. (a) FTIR spectra of PU(PTH) and PU(PTH)-SiO_2-TiO_2 membranes, (b) FTIR spectra at N-H stretching region for PU(PTH) and PU(PTH)-SiO_2-TiO_2 membranes.

This implies that effect of TiO_2 and SiO_2 nanoparticles on polymer matrix is the same and they are mutually exchangeable inside the polymer chains. However, as discussed earlier in FTIR results of the PU(PTH)-TiO_2 and PU(PTH)-SiO_2 MMMs, shift of the NH peak to the lower frequency occurred in the membranes containing TiO_2 and SiO_2 nanoparticles, which can be attributed to the hydrogen bonds between polar groups of Si-OH and Ti-OH in the nanoparticles and NH groups in the polymer. This phenomenon reflects the proper distribution and good dispersion of the nanoparticles in the polymer matrix.

Scanning electron microscope (SEM) was used for morphology observation of MMMs. Figure 9 shows SEM micrographs of the PU(PTH)-TiO_2-SiO_2 MMMs. As shown in Figure 9, the fabricated MMMs are symmetric. Well-dispersed TiO_2 and SiO_2 nanoparticles in the polymer matrix are observable at high-magnified images of the MMMs containing low nanoparticle loading. In particular, by investigating the high magnification micrographs of the MMMs with different SiO_2/TiO_2 ratios, it is obvious that agglomeration of nanoparticles takes place and interfacial voids appear more at the higher silica content. It can be due to SiO_2-SiO_2 interactions that most likely are stronger than the SiO_2-TiO_2 and SiO_2–polymer chains interactions.

As presented in Table 5, glass transition temperature of the PU(PTH)-SiO_2(50)-TiO_2(50) MMM is slightly less than the neat PU(PTH) membrane. The decrease in the glass transition temperature can be due to the increased chain mobility of the polymer surrounding the embedded nanoparticles.

Gas permeability of the PU(PTH) and PU(PTH)-SiO_2-TiO_2 membranes were measured at 10 barg and 30 °C using pure O_2, N_2, CH_4 and CO_2 gases. As shown in Figure 10, gas permeability of all test gases in the MMMs are higher than those in the pure PU(PTH) membrane.

The increase in gas permeability of MMMs containing SiO_2-TiO_2 nanoparticles can be due to the void spaces formed at the polymer/particle interface and the increased free volumes around the embedded nanoparticles that enhanced polymer chain mobility as discussed already in the earlier sections. As shown in Figure 10, permeabilities of all test gases increase as SiO_2/TiO_2 ratio increases and the PU(PTH)-SiO_2(75)-TiO_2(25) sample has the maximum gas permeability values. This effect can be due to the behaviour of silica nanoparticles inside the polymer matrix.

Ideal selectivity of the PU(PTH) and PU(PTH)-SiO_2-TiO_2 membranes is presented in Figure 11. As could be observed in Figure 11, CO_2/CH_4, CO_2/N_2 and O_2/N_2 selectivities of PU(PTH)-SiO_2-TiO_2 MMMs remain nearly constant with only slight increase from the neat PU(PTH). This is most likely because the total nanoparticle solid contents that are kept constant in all MMMs. From the above experimental results, one can conclude that the SiO_2 and TiO_2 nanoparticles have no synergic effect on each other but they behave rather in their own ways. Usually SiO_2 nanoparticles tend to increase permeability more than TiO_2 while TiO_2 nanoparticles increase selectivity more than SiO_2. Therefore, one can improve both permeability and selectivity of MMMs by combining these nanoparticles, as shown in Figure 12 for CO_2/N_2 separation.

4. Conclusions

In this study, three different polyurethanes have synthesized by using two different types of polyol (PTMG and PCL) and two different diisocyanates (IPDI and HMDI) with MOCA as the chain extender. Among those, PTMG containing polyurethane (PU(PTH)) membrane was used for further investigation because of its intrinsically high permeability. The effect of incorporation of SiO_2 and TiO_2 nanoparticles on the gas separation and morphological properties of PU(PTH) membranes was further investigated. Silica nanoparticles have synthesized by sol-gel method while commercial TiO_2 nanoparticles were used. The fabricated mixed matrix membranes (MMMs) have characterized by using FTIR, SEM and DSC. FTIR and SEM results proved that SiO_2 and TiO_2 nanoparticles are well-dispersed inside the polymer matrix (except at high silica contents in the MMMs containing different SiO_2/TiO_2 ratios). DSC analysis showed that the nanoparticles loading decreases the glass transition temperature of MMMs. Gas permeabilities of the neat PU(PTH) and PU(PTH)-TiO_2, PU(PTH)-SiO_2 and PU(PTH)-TiO_2-SiO_2 membranes were measured at 10 barg and 30°C by using pure oxygen, nitrogen, carbon dioxide and methane as test gases. The results showed that the permeabilities of all test gases in the MMMs were higher than those in the neat PU(PTH) membrane. However, the effect of nanoparticles on the selectivity of fabricated MMMs was different. Effect of nanoparticle contents on performance of PU(PTH) membranes was also investigated and it was found that addition of 20 wt. % (solid base) of both TiO_2 and SiO_2 to PU(PTH) matrix could increase permeabilities of all test gases drastically without sacrificing their selectivities.

Nomenclatures

M_w	[g mol^{-1}]	Molecular weight
P	[Barrer]	permeability
q	[cm^{3}s^{-1}]	penetrant volumetric flow rate
l	[cm]	membrane thickness
p_1	[cmHg]	absolute pressures of the feed side
p_2	[cmHg]	absolute pressures of the permeate side
A	[cm2]	effective membrane area
$\alpha_{A/B}$		ideal selectivity
P_A	[Barrer]	permeabilities of penetrants A
P_B	[Barrer]	permeabilities of penetrants B
HBI		hydrogen bonding index
$A_{C=O,bonded}$		absorbance of bonded
$A_{C=O,free}$		free carbonyl groups
T_g	[ºC]	Glass transition temperature
PU(PCH)		PCL containing PU
PU (PTH)		PTMG based polyurethane
PU (PTI)		IPDI containing polyurethane

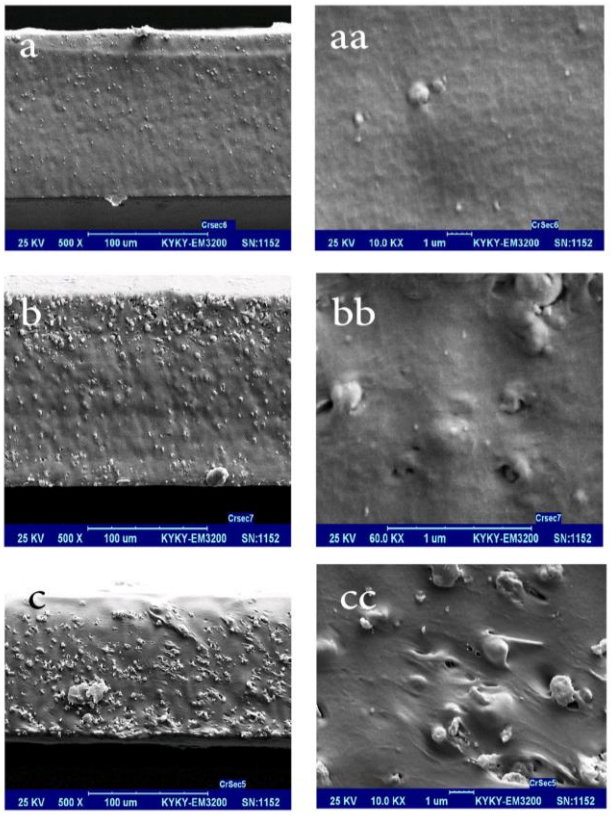

Fig. 9: (a, aa) Cross sectional SEM micrographs of PU(PTH)-SiO_2(25)-TiO_2(75) MMMs, (b, bb) Cross sectional SEM micrographs of PU(PTH)-SiO_2(50)-TiO_2(50) MMMs, (c, cc) Cross sectional SEM micrographs of PU(PTH)-SiO_2(75)-TiO_2(25) MMMs.

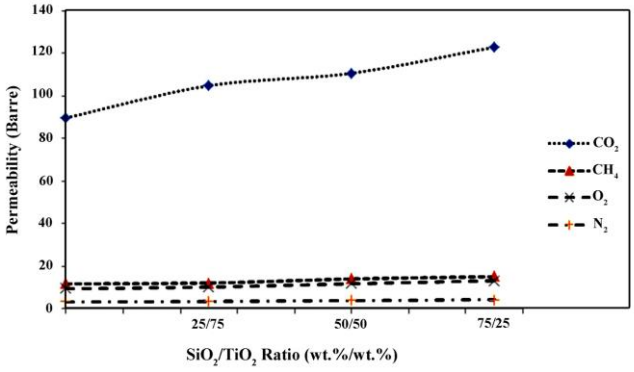

Fig. 10. Gas permeability of the PU (PTH) and PU (PTH)-SiO_2-TiO_2 membrane samples.

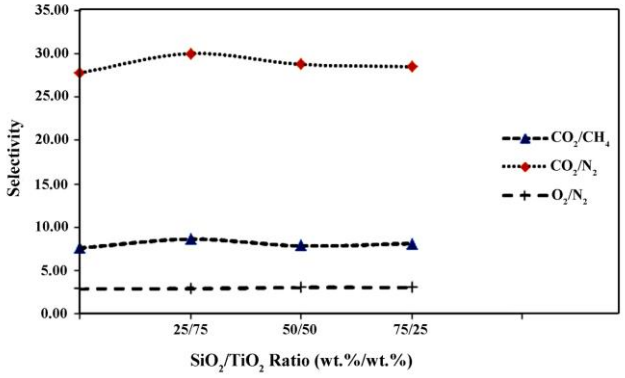

Fig. 11. Ideal selectivity of the PU (PTH) and PU (PTH)-SiO_2-TiO_2 membrane samples.

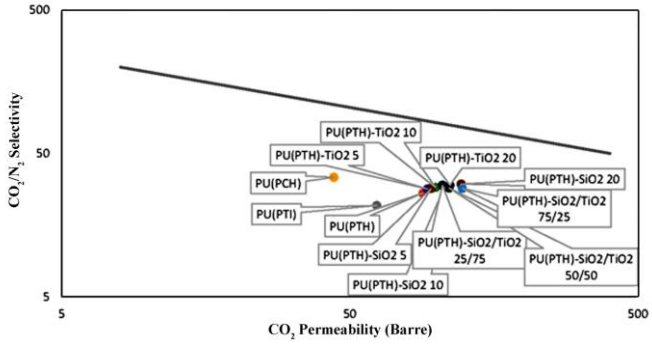

Fig. 12. CO_2/N_2 separation properties of PU(PTH) MMMs containing SiO_2, TiO_2 and SiO_2-TiO_2 nanoparticles on Robeson's upper bound plot.

References

[1] L. M. Robeson, The upper bound revisited, J. Membr. Sci. 320 (2008) 390-400.

[2] R.W Baker, E.L.Cussler, Membrane separation systems- Recent developments and future directions, 1st ed., William Andrew Publishing/Noyes, New Jersey, USA, 1991.

[3] H. Rabiee, S. Meshkat Alsadat, M. Soltanieh, S.A. Mousavi, A. Ghadimi, Gas permeation and sorption properties of poly(amide-12-b-ethyleneoxide)(Pebax1074)/SAPO-34 mixed matrix membrane for CO_2/CH_4 and CO_2/N_2 separation, J. Ind. Eng. Chem. 27 (2015) 223-239.

[4] M. Arruebo, J. Coronas, M. Menéndez, J. Santamaría, Separation of hydrocarbons from natural gas using silicalite membranes , Sep. Purif. Technol. 25 (2001) 275-286.

[5] R.W. Baker, Membrane technology and applications, 2nd ed., John Wiley & Sons, Inc., England, 2004.

[6] T.T. Moore, R. Mahajan, D.Q. Vu, W.J. Koros, Hybrid membrane materials comprising organic polymers with rigid dispersed phases, AIChE. J. 50 (2004) 311-321.

[7] T.T. Moore, W.J. Koros, Non-ideal effects in organic–inorganic materials for gas separation membranes, J. Mol. Struct. 739 (2005) 87-98.

[8] A. Dehghani Kiadehi, A. Rahimpour, M. Jahanshahi, A.A. Ghoreyshi, Novel carbon nano-fibers (CNF)/polysulfone (PSf) mixed matrix membranes for gas separation, J. Ind. Eng. Chem. 22 (2015) 199-207.

[9] D. Bastani, N. Esmaeili, M. Asadollahi, Polymeric mixed matrix membranes containing zeolites as a filler for gas separation applications: A review, J. Ind. Eng. Chem. 19 (2013) 375-393.

[10] M.A. Aroon, A.F. Ismail, T. Matsuura, M.M. Montazer-Rahmati, Performance studies of mixed matrix membranes for gas separation: A review, Sep. Purif. Technol. 75 (2010) 229-242.

[11] J. Bae, J. Lee, C.S. Park, O.S. Kwon, C.S. Lee, Fabrication of photo-crosslinkable polymer/silica sol–gel hybrid thin films as versatile barrier films, J. Ind. Eng. Chem. 38 (2016) 61-66.

[12] M. Naghsh, M. Sadeghi, A. Moheb, M.P. Chenar, M. Mohagheghian, Separation of ethylene/ethane and propylene/propane by cellulose acetate–silica nanocomposite membranes, J. Membr. Sci. 423-424 (2012) 97-106.

[13] S.M. Davoodi, M. Sadeghi, M. Naghsh, A. Moheb, Olefin–paraffin separation performance of polyimide Matrimid®/silica nanocomposite membranes, RSC Adv. 6 (2016) 23746-23759.

[14] M. Sadeghi, M.M. Talakesh, B. Ghalei, M.R. Shafiei, Preparation, characterization and gas permeation properties of a polycaprolactone based polyurethane-silica nanocomposite membrane, J. Membr. Sci. 427 (2013) 21-29.

[15] M. Moaddeb, W.J. Koros, Gas transport properties of thin polymeric membranes in the presence of silicon dioxide particles, J. Membr. Sci. 125 (1997) 143-163.

[16] T.C. Merkel, B.D. Freeman, R.J. Spontak, Z. He, I. Pinnau, P. Meakin, A.J. Hill, Ultrapermeable, reverse-selective nanocomposite membranes, Science 296 (2002) 519-522.

[17] D.W. Lee, B.R. Yoo, Advanced silica/polymer composites: Materials and applications, J. Ind. Eng. Chem. 38 (2016) 1-12.

[18] J.H. Kim, Y.M. Lee, Gas permeation properties of poly(amide-6-b-ethylene oxide)–silica hybrid membranes, J. Membr. Sci. 193 (2001) 209-225.

[19] C. Joly, S. Goizet, J.C. Schrotter, J. Sanchez, M. Escoubes, Sol-gel polyimide-silica composite membrane: Gas transport properties, J. Membr. Sci. 130 (1997) 63-74.

[20] I. Pinnau, Z. He, Filled superglassy membrane, US Patent 6 316 684, 2001.

[21] Z. He, I. Pinnau, A. Morisato, Nanostructured poly(4-methyl-2-pentyne)/silica hybrid membranes for gas separation, Desalination 146 (2002) 11-15.

[22] J. Ahn, W.J. Chung, I. Pinnau, M.D. Guiver, Polysulfone/silica nanoparticle mixed-matrix membranes for gas separation, J. Membr. Sci. 314 (2008) 123-133.

[23] M. Sadeghi, H.T. Afarani, Z. Tarashi, Preparation and investigation of the gas separation properties of polyurethane-TiO_2 nanocomposite membranes, Korean J. Chem. Eng. 32 (2015) 97-103.

[24] S. Matteucci, V.A. Kusuma, D. Sanders, S. Swinnea, B.D. Freeman, Gas transport in TiO_2 nanoparticle-filled poly(1-trimethylsilyl-1-propyne), J. Membr. Sci. 307 (2008) 196-217.

[25] Y. Kong, H. Du, J. Yang, D. Shi, Y. Wang, Y. Zhang, W. Xin, Study on polyimide/TiO_2 nanocomposite membranes for gas separation, Desalination 146 (2002) 49-55.

[26] Q. Hu, E. Marand, S. Dhingra, D. Fritsch, J. Wen, G. Wilkes, Poly(amide-imide)/TiO_2 nano-composite gas separation membranes: Fabrication and characterization, J. Membr. Sci. 135 (1997) 65-79.

[27] H. Xiao, Z. H. Ping, J.W. Xie, T.Y. Yu, Permeation of CO_2 through polyurethane, J. Appl. Polym. Sci. 40 (1990) 1131-1139.

[28] P.M. Knight, D.J. Lyman, Gas permeability of various block copolyether-urethanes, J. Membr. Sci. 17 (1984) 245-254.

[29] N. Cao, M. Pegoraro, F. Bianchi, L. Di Landro, L. Zanderighi, Gas transport properties of polycarbonate–polyurethane membrance, J. Appl. Polym. Sci. 48 (1993) 1831-1842.

[30] A. Wolińska-Grabczyk, Effect of the hard segment domains on the permeation and separation ability of the polyurethane-based membranes in benzene/cyclohexane separation by pervaporation, J. Membr. Sci. 282 (2006) 225-236.

[31] A. Pournaghshband, B. Ghalei, R. Bagheri, Y. Kinoshita, H. Kitagawa, E. Sivaniah, M. Sadeghi, Polyurethane gas separation membranes with ethereal bonds in the hard segments, J. Membr. Sci. 513 (2016) 58-66.

[32] J.M. Yang, H.T. Lin, S.J. Yang, Evaluation of poly(N-isopropylacrylamide) modified hydroxyl-terminated polybutadiene based polyurethane membrane, J. Membr. Sci. 258 (2005) 97-105.

[33] A. Wolińska-Grabczyk, A. Jankowski, Gas transport properties of segmented polyurethanes varying in the kind of soft segments, Sep. Purif. Technol. 57 (2007) 413-417.

[34] A. Wolińska-Grabczyk, W. Bednarski, A. Jankowski, S. Waplak, Permeable domains of segmented polyurethanes studied with paramagnetic spin probe, Polymer, 45 (2004) 791-798.

[35] L.S. Teo, J.F. Kuo, C.Y. Chen, Study on the morphology and permeation property of amine group-contained polyurethanes, Polymer, 39 (1998) 3355-3364.

[36] E. Ameri, M. Sadeghi, N. Zarei, A. Pournaghshband, Enhancement of the gas separation properties of polyurethane membranes by alumina nanoparticles, J. Membr. Sci. 479 (2015) 11–19.

[37] H.B. Park, Y.M. Lee, Separation of toluene/nitrogen through segmented polyurethane and polyurethane urea membranes with different soft segments, J. Membr. Sci. 197 (2002) 283-296.

[38] M. Khoshkam, M. Sadeghi, M. Pourafshari, M. Naghsh, M.J. Namazifard, M.R. Shafiei, Synthesis, characterization and gas separation properties of novel copolyimide membranes based on flexible etheric–aliphatic moieties, RSC Adv. 6 (2016) 35751-35763.

[39] A. Khosravi, M. Sadeghi, H. Zare and M. Talakesh, Polyurethane-Silica Nanocomposite Membranes for Separation of Propane/Methane and Ethane/Methane, Ind. Eng. Chem. Res. 53 (2014) 2011-2021.

[40] A. Pournaghshband, M. Sadeghi, A.H. Saeedi, M.A. Aravand, Enhancement of the gas separation properties of polyurethane membrane by epoxy nanoparticles, J. Ind. Eng. Chem. 44 (2016) 67-72.

[41] T.T. Moore, W.J. Koros, Gas sorption in polymers, molecular sieves, and mixed matrix membranes, J. Appl. Polym. Sci. 104 (2007) 4053–4059.

[42] H.F. Naguib, M.S. Abdel Aziz, G.R. Saad, Synthesis, morphology and thermal properties of polyurethanes nanocomposites based on poly(3-hydroxybutyrate) and organoclay, J. Ind. Eng. Chem. 19 (2013) 56-62.

[43] S. Pourjafar, A. Rahimpour, M. Jahanshahi, Synthesis and characterization of PVA/PES thin film composite nanofiltration membrane modified with TiO_2nanoparticles for better performance and surface properties, J. Ind. Eng. Chem. 18 (2012) 1398-1405.